Human Parafoveal Capillary Vascular Anatomy and Connectivity Revealed by Optical Coherence Tomography Angiography

Peter L. Nesper and Amani A. Fawzi

The Department of Ophthalmology, Feinberg School of Medicine, Northwestern University, Chicago, Illinois, United States

Correspondence: Amani A. Fawzi, Department of Ophthalmology, Feinberg School of Medicine, Northwestern University, 645 N. Michigan Avenue, Suite 440, Chicago, IL 60611, USA; afawzimd@gmail.com.

Submitted: May 2, 2018
Accepted: July 7, 2018

Citation: Nesper PL, Fawzi AA. Human parafoveal capillary vascular anatomy and connectivity revealed by optical coherence tomography angiography. *Invest Ophthalmol Vis Sci.* 2018;59:3858–3867. https://doi.org/10.1167/iovs.18-24710

Purpose. To assess the connection among arterioles, venules, and capillaries in three retinal capillary plexuses using optical coherence tomography angiography (OCTA).

Methods. This was a prospective, cross-sectional, observational study including 20 eyes of 10 healthy subjects. En face and cross-sectional OCTA images were segmented to study the superficial (SCP), middle (MCP), and deep capillary plexuses (DCP). Using thin slabs and manual segmentation within the three plexuses, we examined the connections between the large-caliber superficial vessels within a 3×3 mm^2 OCTA scan (arterioles and venules) and the smaller capillaries in each plexus.

Results. Twenty eyes of 10 healthy subjects (5 females; average age of 30.8 ± 6.3 years) were included in the analysis. We identified vascular interconnections linking the superficial arterioles and venules with capillaries in each plexus (SCP, MCP, and DCP). We found capillaries in the DCP crossed the horizontal raphe.

Conclusions. Our findings show that each of the three capillary plexuses in the parafovea has its own feeding arteriolar supply and draining venules, supporting a physiologic model in which each plexus controls its own oxygenated blood supply to match the metabolic needs of each distinct retinal neurovascular unit.

Keywords: optical coherence tomography angiography, OCT, OCTA, macula, retina, macular capillary plexus

The morphology and function of the retinal capillary layers are coupled with the metabolic demands of the neuronal retina, which require efficient delivery of oxygen and metabolites, along with efficient waste removal. Understanding the distribution and morphometry of the retinal vasculature is key to studying the pathophysiology of retinal dysfunction in ischemia. Histological studies of the human parafovea have identified three distinct capillary layers: the superficial (SCP), middle (MCP), and deep capillary plexus (DCP),[1] with a fourth vascular layer, the radial peripapillary capillaries, mainly located in the superficial nerve fiber layers surrounding the optic nerve.[2] Our understanding of the development and anatomy of the human retinal vascular plexuses thus far has largely stemmed from histological evidence in the primate retina.[3–7] More recently, optical coherence tomography angiography (OCTA),[8–11] speckle variance OCT,[12] and several instruments using adaptive optics have confirmed the trilaminar capillary layout of the parafovea in humans.[13–15]

Since the inception of OCTA, a number of models have been proposed to relate the connections among the retinal vascular plexuses, inviting debates regarding their functions. Using OCTA and segmenting two retinal capillary plexuses (instead of three), Bonnin et al.[16] proposed that the SCP was composed of horizontal, alternating arterioles and venules surrounding the foveal avascular zone, and the DCP was composed of polygonal units of capillary vortices with capillaries converging toward a venous connecting channel in its epicenter. Park et al.[8] were first to segment the MCP using OCTA and similarly showed the presence of capillary vortices in the DCP. Drawing conclusions from these and other studies, Garrity and colleagues[17] questioned whether the SCP and MCP have independent arteriolar supply and venular drainage; instead, these authors proposed a serial organization of the retinal vasculature with the venous drainage of the entire parafovea draining primarily into the DCP. Using projection-resolved OCTA (PR-OCTA), which reduces artifacts and provides a more detailed three-dimensional view of the capillaries, Campbell et al.[9] found that arterioles and venules connect to capillaries in each capillary layer and predicted these connections occur in an alternative parallel or "hammock" model, wherein each neurovascular/capillary layer operates as an independent unit with its own arteriolar supply and venous drainage. This model would support the generally accepted neurovascular unit, with independent control of the capillary layers that match their neuronal needs.[18,19] Specifically, using elegant high-resolution experiments in the rodent retina, Biesecker and colleagues have shown that the retinal capillary layers are differentially regulated, both at the arteriolar and capillary levels,[18] with MCP capillaries being maximally dilated during flicker stimulation, compared with the SCP capillaries which show decreased flow under the same conditions.[19] In healthy human subjects, Hagag and colleagues have recently shown that exposure to hyperoxia maximally constricted the DCP with minimal effect on the other capillary layers.[20] This intricate, precise, and differential regulation of these capillary layers would suggest an indepen-

dent neurovascular unit at each capillary plexus, favorably supporting the parallel connectivity model.

Notably, these previous OCTA studies used a commercial OCTA system with split-spectrum amplitude-decorrelation angiography (SSADA) software.[21] In general, OCTA devices extract angiographic information of blood cell movement by comparing OCT signal changes between two or more consecutive B-scans at the same location in the retina. The SSADA algorithm compares the amplitude between two consecutive B-scans and splits the OCT spectrum into 11 sub-bands, which improves the signal-to-noise ratio at the expense of lower axial resolution of the flow angiogram (~20 μm).[9,21,22]

In this study, we wanted to explore whether using a different OCTA algorithm with better axial resolution could provide an improved distinction of the retinal vascular connections. The Zeiss Angioplex (Zeiss Meditec, Inc., Dublin, CA, USA) is based on the optical microangiography (OMAG) software, which compares amplitude and phase differences among four consecutive B-scans in a 3 × 3 mm^2 cube.[23,24] Since the OMAG algorithm does not split the OCT spectrum into sub-bands, it theoretically provides a higher axial resolution of approximately 5 μm in tissue.[25] In the current study, we capitalized on this particular feature of the Angioplex OCTA system to facilitate the visualization of connections among the three parafoveal capillary plexuses in healthy subjects.

Methods

This was a prospective analysis of healthy subjects recruited in the Department of Ophthalmology at Northwestern University in Chicago, Illinois, between December 2017 and January 2018. This study was approved by the Institutional Review Board of Northwestern University, followed the tenets of the Declaration of Helsinki and was performed in accordance with the Health Insurance Portability and Accountability Act regulations. Written informed consent was obtained from all participants.

Study Sample

Inclusion criteria included subjects with no history of ocular disease or systemic diseases that may affect the retinal vasculature, such as hypertension. Only eyes that had OCTA images without large movement or shadow artifacts were considered eligible. Exclusion criteria included eyes with a history of surgical retinal repair or those with any retinal disease, such as high myopia (over −7 diopters). To avoid optical artifacts that may compromise OCTA image quality, we also excluded patients with evidence of cataracts above nuclear opalescence grade three or nuclear color grade three.[26] Electronic medical records were reviewed to extract demographic and clinical information.

OCTA Imaging

We acquired 3 × 3 mm^2 OCTA scans centered on the fovea using the commercially available Zeiss Cirrus HD-OCT 5000–2328 (Zeiss Meditec, Inc.) with OMAG Angioplex (software version 9.5.0.8712).[24] This device has an A-scan rate of 68,000 scans per second with a light source with a central wavelength of 840 nm and a full-width at half maximum of 90 nm.[23,24] The 3 × 3 mm^2 OMAG scanning pattern is achieved by repeating B-scan acquisition four times at each retinal position in the slow *y*-axis (each of the 245 total B-scans, separated by 12.5 μm) with 245 A-scans per B-scan in the fast *x*-axis.[25] A line scan ophthalmoscope with real-time retinal tracking reduces motion artifacts.[27,28] The 3 × 3 mm^2 en face angiograms centered on the fovea were exported at 429 × 429 pixel resolution. We included scans only if they had high image quality as indicated by signal strength of 7 or higher.

Image Analysis

The SCP was defined as the vascular plexus located in the nerve fiber and ganglion cell layers. The MCP was defined as the capillary plexus located at the boundary of the inner plexiform layer (IPL) and inner nuclear layer (INL) and the DCP was defined as the capillary plexus at the boundary of the INL and outer plexiform layer (OPL).[1,4] Using Angioplex software, the SCP was segmented from the inner limiting membrane to 55 μm above the IPL, the MCP was segmented from 55 to 6 μm above the IPL, and the DCP was segmented from 6 μm above the IPL to 50 μm below the IPL. We activated the manual "Remove Projections" option in the Angioplex software for all analyses, which uses additive mixing of overlying vessels to reduce projection artifacts in lower layers.[29] One grader (PLN) analyzed OCTA images for vascular characteristics within the SCP, MCP, and DCP. Using en face OCTA, the presence or absence of feeding arterioles and draining venules to and from each of the layers was assessed by tracing the connection between capillaries in a given layer to their arteriole/venule parent vessels in the SCP. We defined parent vessels as the arterioles or venules with the greatest diameters in the SCP within the 3 × 3 mm^2 OCTA scan centered on the fovea. Cross-sectional OCTA was used to confirm the axial location of vessels within the retina. Arterioles in the SCP were distinguished from venules based on the larger capillary-free zone surrounding arterioles. For DCP analysis, we additionally traced all the capillaries radiating out from the "vortex" to their SCP connections in two different eyes. Image masks of the superficial arterioles and venules were pseudo-colored using Adobe Photoshop (Version 13.0.4; Adobe Systems, Inc., San Jose, CA, USA).

Results

Twenty eyes of 10 healthy subjects were included and analyzed. Of these subjects, five (50%) were female with an overall average age of 30.8 ± 6.3 years. Study participant race/ethnicity included White ($n = 6$), Hispanic ($n = 2$), and Asian ($n = 2$). The SCP, MCP, and DCP were successfully segmented in each eye (Fig. 1). We found that arterioles and venules within the SCP had vascular connections to all three capillary layers (SCP, MCP, and DCP). In all eyes, we found that SCP arterioles were consistently more anterior (closer to the vitreous) than adjacent venules (Fig. 2), which has been previously described in histological studies.[30]

Arteriolar connections to the SCP and MCP capillaries were more easily identified than those to the DCP. For DCP connections, vertically diving vessels could be easily confounded by flow projection artifact. Therefore, by focusing on vascular channels with an oblique intraretinal trajectory, we were able to confirm direct connections between the SCP arterioles and the DCP (Figs. 3, 4). Supplementary Figure S1 shows a video fly-through revealing an arteriole diving into the DCP.

The DCP harbored vortices with central channels that drained directly into the SCP venules. Similarly, capillaries within the SCP and MCP drained directly into SCP venules (Figs. 5, 6). When focusing on DCP vortices, we found that the capillaries radiating out from these central DCP vortices connected to both arteriolar and venular vessels (in the SCP)

Investigative Ophthalmology & Visual Science

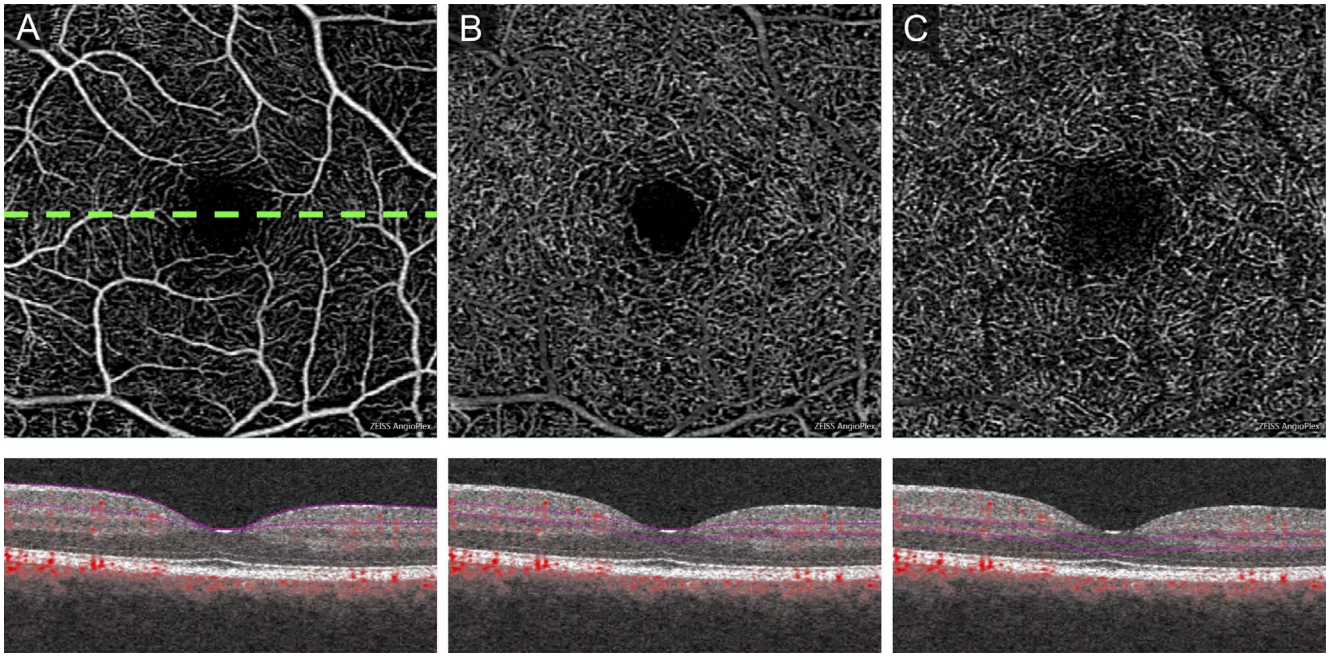

Figure 1. Segmentation of three distinct capillary plexuses in the parafovea using Angioplex OCTA. (**A**) En face image of the superficial capillary plexus and cross-section below with *purple segmentation boundary lines* and *red flow overlay*. Arterioles on the en face image have larger capillary-free zones surrounding the vessel compared with venules. *Dotted line* shows location of cross-sections for (**A–C**). (**B**) En face image of the middle capillary plexus and cross-section below with segmentation and flow overlay. (**C**) En face image of the DCP and cross-section below with segmentation and flow overlay. Dark lines can be seen on the en face image and are a result of the removal of projection artifacts from larger overlying blood vessels.

via connecting channels, as well to other vortices in the DCP (Figs. 4, 7). Interestingly, we found that vortices had connections that crossed the horizontal raphe within the DCP (Figs. 7, 8). Supplementary Figures S2 and S3 show fly-through videos of Figures 7 and 8, respectively. A schematic of our current understanding of the parafoveal capillary connectivity is illustrated in Figure 9.

Discussion

Capitalizing on the higher axial resolution of the OMAG software, we identified distinct vascular connections from large-caliber arterioles and venules in the SCP to each of the three retinal capillary plexuses (SCP, MCP, and DCP) in healthy subjects. We provide further evidence for the existence of vortices in the DCP, which drain into central conduits that directly connect to venules in the SCP. We found that capillaries radiating out from these central vortices connect to arteriolar SCP vessels, as well as to other vortices in the DCP (and through them to other venules in the SCP) with connections that peculiarly crossed the horizontal raphe. Although previous models of connectivity and function of the three parafoveal capillary plexuses have provided important insight, our data suggest there are additional qualities of these capillary connections that are important to consider.[8,9,16,17] Based on the current study findings, we present an alternative model that is a hybrid of the "hammock" model,[9] which incorporates elements from our results and other studies.[8,16,17,31]

The basic premise of the "hammock" model is that each of the three plexuses has its own arteriolar supply and venular drainage, which would theoretically allow each neurovascular unit to have independent control of its vascular supply under physiologic conditions. This model is supported by developmental and physiological studies, including primate developmental studies in which the deeper vasculature develops from sprouting of the more superficial layers via angiogenesis.[3,4] Specifically, capillaries sprout from the SCP and form a new layer of vessels at the IPL/INL border (MCP) and INL/OPL border (DCP).[3,4,32] This occurs when leading glia and neurons sense hypoxia and express vascular endothelial growth factor, which guides and stimulates endothelial cell proliferation.[3] From histological studies in humans, we know that the MCP lies at the boundary of IPL and inner portion of the INL, colocalizing with the bipolar cell processes and amacrine cells in close proximity to the high oxygen demand of the IPL synapses,[33] whereas the DCP lies at the boundary of the deep INL and OPL, colocalizing with horizontal cells and close to the OPL synapses.[1,2] Retinal oxygen measurement experiments in animal models have determined that the dominant oxygen consumers of the inner retina are located in the plexiform layers (IPL and OPL), presumably in the mitochondria-rich synapses.[34–38] The high oxygen demand of the plexiform layers suggests the need for highly oxygenated (arteriolar) blood supply in these layers. Indeed, oxygen-sensitive microelectrode studies in primates, cats, and rats have shown peaks in oxygen tension in both plexiform layers.[39–42] Thus, from a physiological standpoint, each capillary plexus likely receives its own highly oxygenated arteriolar blood supply. Indeed, using angiography and histological techniques in primates, Snodderly et al.[6,7] showed arteriolar supply to all three capillary plexuses. These studies lend support to the idea that each of the three plexuses has its own arteriolar supply and venular drainage, allowing the individual neuronal layers to control their supply according to their specialized metabolic activities.

Several investigators have proposed a serial model of connectivity between the arterioles, starting at the SCP, to the MCP, then finally draining through the DCP and from DCP directly into the SCP venules.[17] They proposed that the SCP and MCP do not function as distinct capillary units with

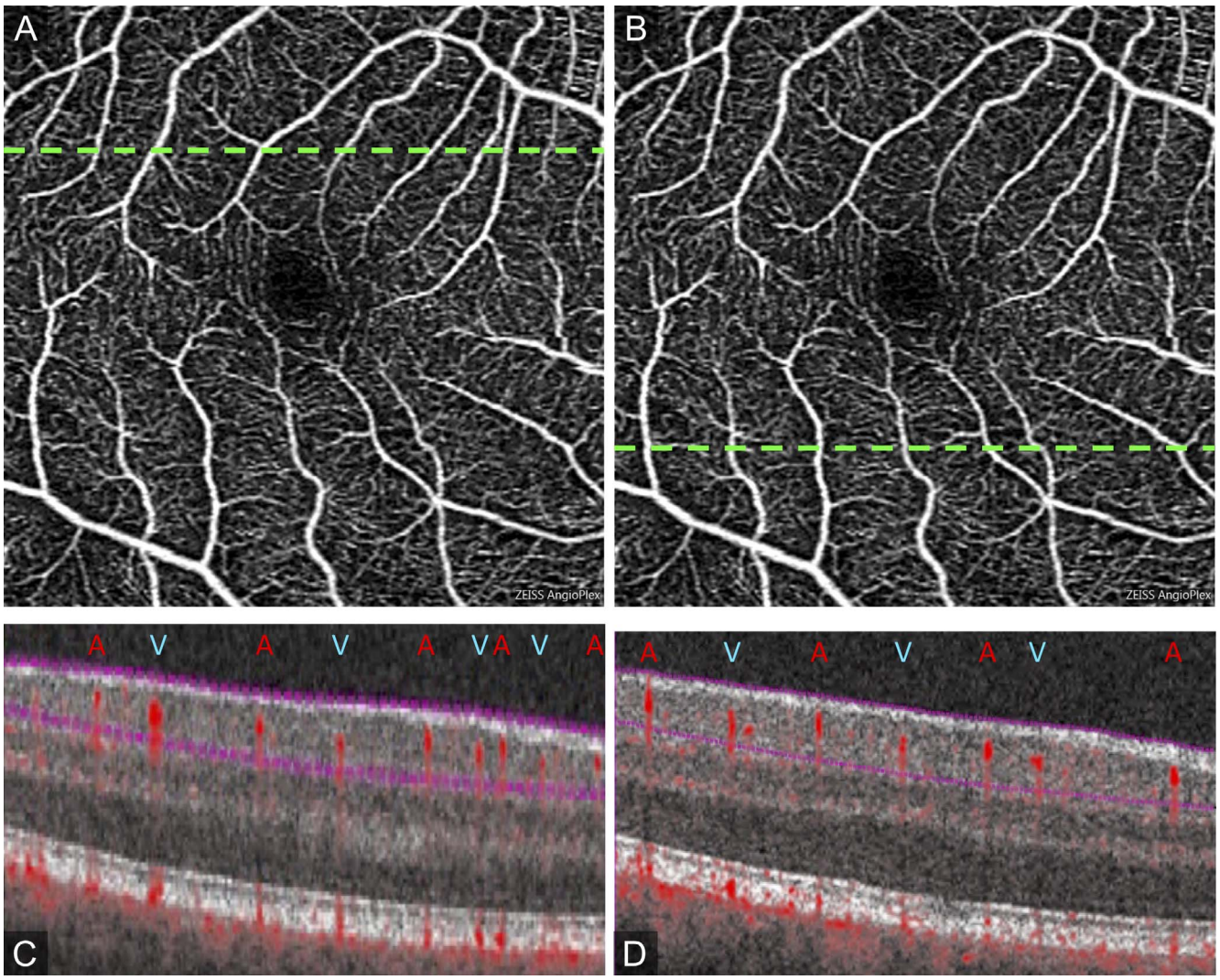

Figure 2. Arterioles are located more superficially than adjacent venules in the superficial retina. (**A**, **B**) En face OCTA with *blue lines* indicating the location of corresponding cross-sections below. *Dotted lines* show locations of cross-sections. Compared with venules, arterioles have a wider capillary-free zones along them, which is seen best on the en face angiogram in (**A**) and (**B**). (**C**, **D**) The arterioles (*red A*) are located more superficially (anteriorly) compared with adjacent venules (*blue V*).

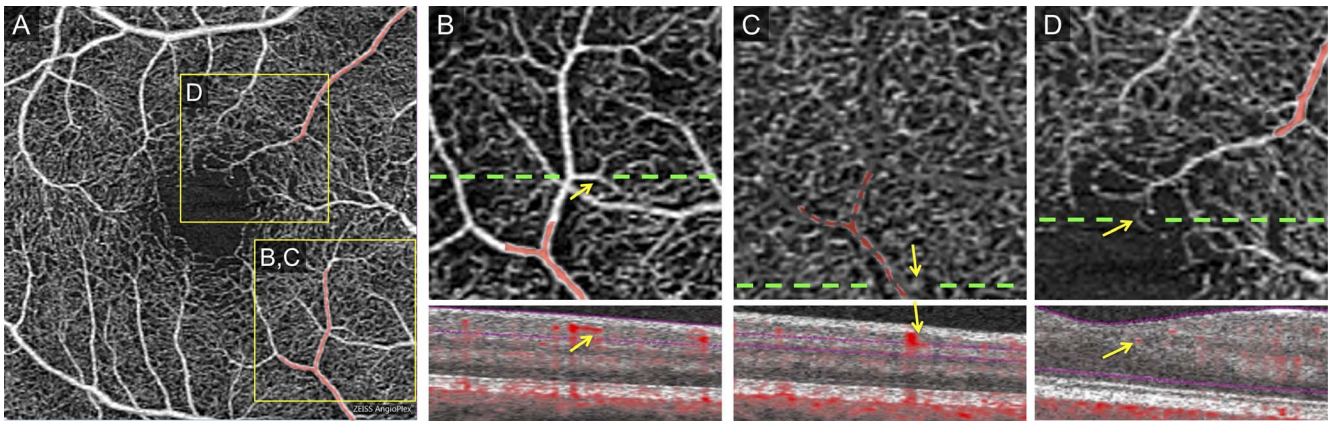

Figure 3. Arterioles connect to capillaries in all three macular capillary plexuses. (**A**) En face OCTA of the full retinal thickness with *yellow boxes* showing location of enlarged insets. Arterioles of interest are pseudo-colored *red*. (**B**) En face (*top*) and cross-sectional (*bottom*) OCTA inset of the SCP showing an arteriole (*red*) connecting to the SCP capillaries (*arrow*). *Dotted lines* show locations of cross-sections for (**B–D**). (**C**) En face (*top*) and cross-sectional (*bottom*) OCTA inset of the MCP showing the same superficial arteriole (*red*) connecting to the MCP capillaries (*arrow*). (**D**) En face (*top*) and cross-sectional (*bottom*) OCTA inset of the full retinal thickness showing another arteriole (*red*) terminating at the border of the foveal avascular zone in the DCP at the border of the INL and OPL (*arrow*).

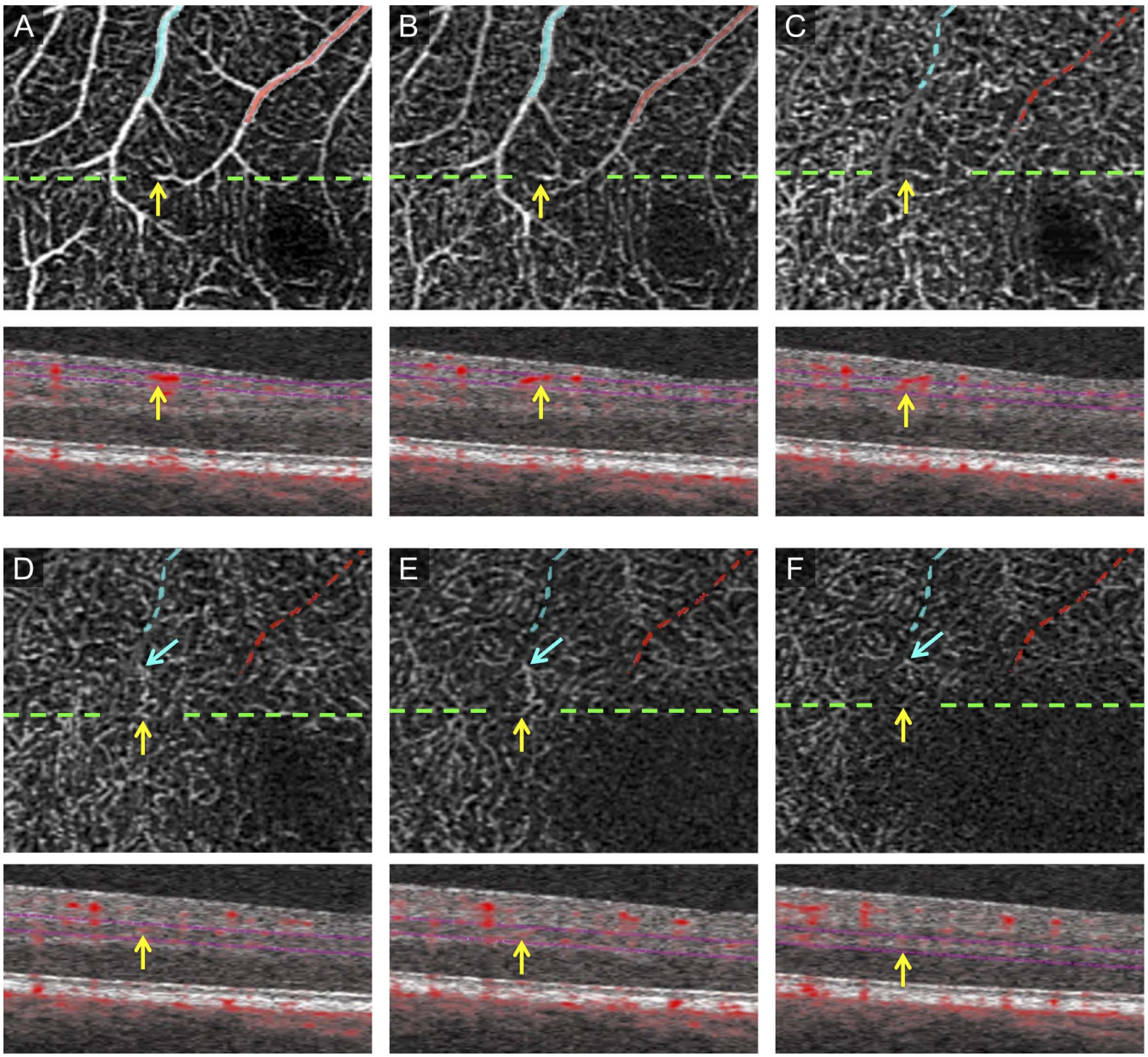

FIGURE 4. Arteriole terminates in the DCP. (**A–F**) En face OCTA with cross-sectional OCTA below showing *segmentation boundary lines* and *red flow overlay. Dotted lines* show locations of cross-sections for (**A–F**). The arteriole and venule of interest are pseudo-colored *red* and *blue*, respectively. We show 30-μm-thick slabs that start superficially (**A**) and track the arteriolar branches as they descend into the DCP (**F**). *Yellow arrows* point to the descending arteriole. (**E**, **F**) In the DCP, the arteriole (*yellow arrow*) makes a connection to a venous vortex (*blue arrow*) via DCP capillaries.

independent venous outflow, but rather that most venous drainage of the parafovea would primarily occur via the DCP. This model was proposed based on OCTA studies demonstrating the vortex-like capillaries in the DCP, which drain centrally into the larger venules located in the SCP.[8,16,31,43] There is excellent evidence for the anatomical arrangement of capillaries in peculiar spider-like "vortices" in the DCP, in the current, as well as other OCTA[14,15] and histologic studies.[4,5,44] However, the presence of the central venular connection of these vortices should not be conflated with a primary venous function of the DCP, given the requirement for high oxygen in the OPL. Physiologically, it seems the high demand and consumption of oxygen in the OPL precludes the possibility that this capillary layer (DCP) would consist exclusively of a venular drainage basin, carrying deoxygenated blood. Further contradicting the DCP as primary venous outflow for the parafovea, our data show independent venous outflow for the SCP and MCP (Figs. 5, 6). In addition, we found arteriolar connections that directly traverse the inner retinal layers and terminate in the DCP capillaries at the border of the INL and OPL (Figs. 3, 4). Indeed, tracing the spider-like vortex capillaries in the DCP, we found that these connect to arterioles in the SCP (Figs. 4, 7, 8).

Curiously, several authors have noted that collateral formation in venous occlusive disease involves dilation of DCP channels in rodent models and, more recently, in human branch vein occlusions.[45,46] This finding would suggest that the DCP route offers the path of least resistance for dilation and collateral formation, serving as a bypass route for obstruction at the level of the larger SCP venules. However,

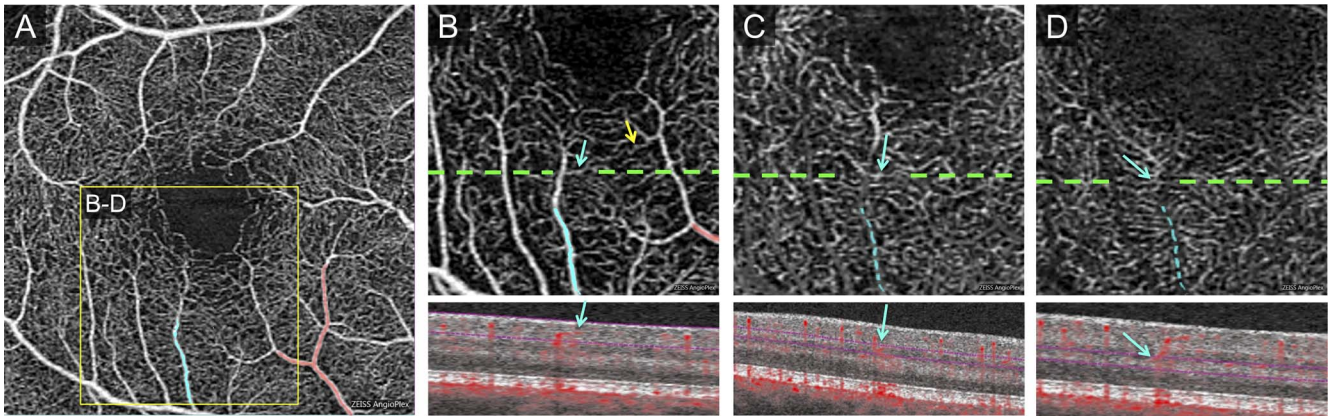

Figure 5. Venous channels connect all three macular capillary plexuses to the superficial venules. (**A**) En face OCTA of the full retinal thickness with *yellow box* showing location of enlarged inset. Venule of interest is pseudo-colored *blue* while arteriole of interest is pseudo-colored *red*. (**B**) En face (*top*) and cross-sectional (*bottom*) OCTA inset of the SCP showing arterio-venous capillary connections at the SCP (*arrows*). *Dotted lines* show locations of cross-sections for (**B–D**). (**C**) En face (*top*) and cross-sectional (*bottom*) OCTA inset of the MCP showing a venule (*blue*) connecting to the MCP capillaries (*arrow*). (**D**) En face (*top*) and cross-sectional (*bottom*) OCTA inset of the DCP showing the same venule (*blue*) connecting to the DCP capillaries (*arrow*).

this pathologic adaptation to venous outflow obstruction does not necessarily mean that the same route is the pathway for physiologic venous outflow. We provide further evidence that vortices in the DCP are connected to arteriolar as well as venular channels (Figs. 4, 7). One unique characteristic that we have identified as potentially explaining their involvement in collateral formation is the presence of vortex channels that cross the horizontal raphe in the DCP (Figs. 7, 8). We propose that these unusual crossing channels would offer a highly interconnected and alternative pathway of least resistance for collateral formation, in the event of branch venous occlusive disease. This peculiar organization of the DCP would offer an alternative explanation for the excellent observations made by previous authors.[45,46]

The vortex nature of capillaries in the DCP does not preclude the possibility of the hammock configuration for the DCP; neither do anastomoses between the plexuses. These are important findings that complement our understanding of the complex connectivity of the three retinal plexuses of the parafovea. In a histological study of primate retina, Snodderly et al.[6] found that venous outflow paths showed conversion of several capillaries from different levels onto the same large SCP venule. In contrast, most retinal vascular anatomy (including the arteriolar supply) was dichotomous.[6] These single-vessel precapillary arteriolar connections originating from SCP arterioles and destined to supply the deeper layers would be more difficult to identify in OCTA, especially when using algorithms that have lower axial resolution. In addition, these channels are particularly challenging to differentiate from projection artifact. In contrast, the central vortex connection to venules, by virtue of its flat configuration and the convergence of many capillaries, is generally more conspicuous and easier to trace to its draining venule.

Based on the current study, as well as previous anatomic and physiologic studies, we propose that each capillary plexus receives its own arteriolar supply as well as connecting to SCP draining venules. Although this generally supports the basic premise of the "hammock" model proposed by Campbell et al.,[9] it adds several elements to that model. Importantly, our model incorporates capillary anastomoses (direct connections)

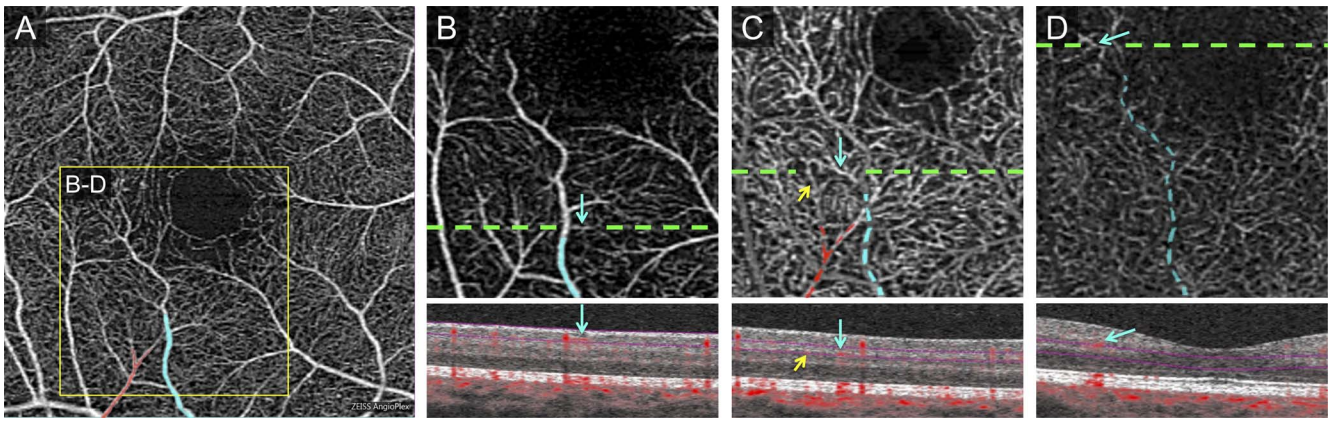

Figure 6. Venular connections to capillaries in all three macular plexuses. (**A**) En face OCTA of the full retinal thickness with *yellow box* showing location of enlarged inset. Venule of interest is pseudo-colored *blue* while arteriole of interest is pseudo-colored *red*. (**B**) En face (*top*) and cross-sectional (*bottom*) OCTA inset of the SCP showing the venule (*blue*) connecting to the SCP capillaries (*arrow*). *Dotted lines* show locations of cross-sections for (**B–D**). (**C**) En face (*top*) and cross-sectional (*bottom*) OCTA inset of the MCP showing a venule (*blue*) connecting to the MCP capillaries (*arrow*). The connection of these capillaries to the venule is seen on the en face image and these MCP capillaries also form connections (*yellow arrow*) with adjacent arterioles (*red*). (**D**) En face (*top*) and cross-sectional (*bottom*) OCTA inset of the DCP showing venule (*blue*) terminating in the DCP near the foveal avascular zone (*arrow*).

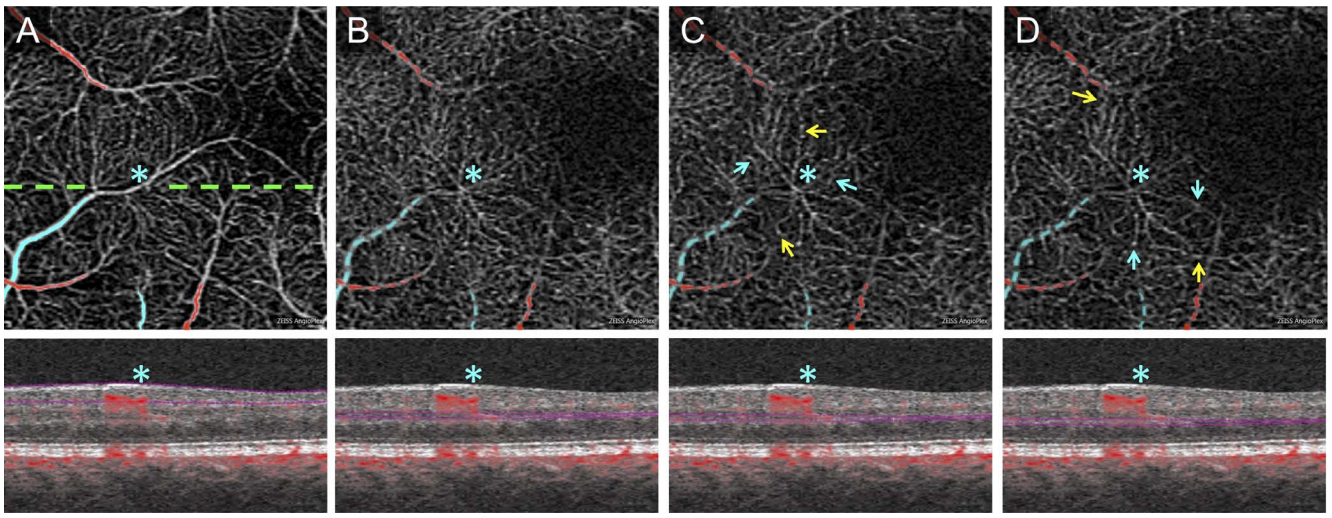

Figure 7. The "vortex" system in the DCP connects to several arterioles and venules with connections that cross the horizontal raphe. (**A**) En face OCTA of the SCP with arterioles (pseudo-colored *red*) and venules (pseudo-colored *blue*). Cross-sectional OCT below each angiogram with *purple segmentation boundaries* and *red flow overlay. Dotted line* shows location of cross-sections for (**A–D**). *Asterisks* highlight central channel of the "vortex" system. (**B–D**) Thin slabs (30 μm) of the DCP taken progressively deeper into the retina. (**B**) Central conduit of the "vortex" system connecting to a venule (*asterisk*). (**C**, **D**) The vortex fans out in a radial fashion with connections to both arterioles (*yellow arrows*) and venules (*blue arrows*). Note that these connections peculiarly cross the horizontal raphe in the DCP (**D**).

between each of the three plexuses.[47] Using an OCTA microscope in anesthetized rats, Leahy et al.[47] found that most anastomoses occurred between the MCP and DCP with a dense anastomotic vessel density of 253 mm^2, compared with 77.2 mm^2 between SCP and MCP, and 26.9 mm^2 between SCP and DCP. The nature of these anastomoses (whether arteriolar or venular) has not been well characterized and their visualization is technically challenging for OCT technology given their axial path (parallel to the OCT beam). Anastomoses between each of the layers have been shown in close proximity to arterioles and venules.[3,5,6,46] Paques and colleagues[46] used confocal microscopy of fluorescein-labeled rodent vessels to show that a greater proportion of anastomotic vessels were arteriolar, directing flow from the SCP toward the deeper layers.

In addition to illustrating these anastomoses, our schematic (Fig. 9) demonstrates the vortex arrangement of capillaries in the DCP (discussed above), arterioles located on a more superficial plane compared with venules,[30] and the three-

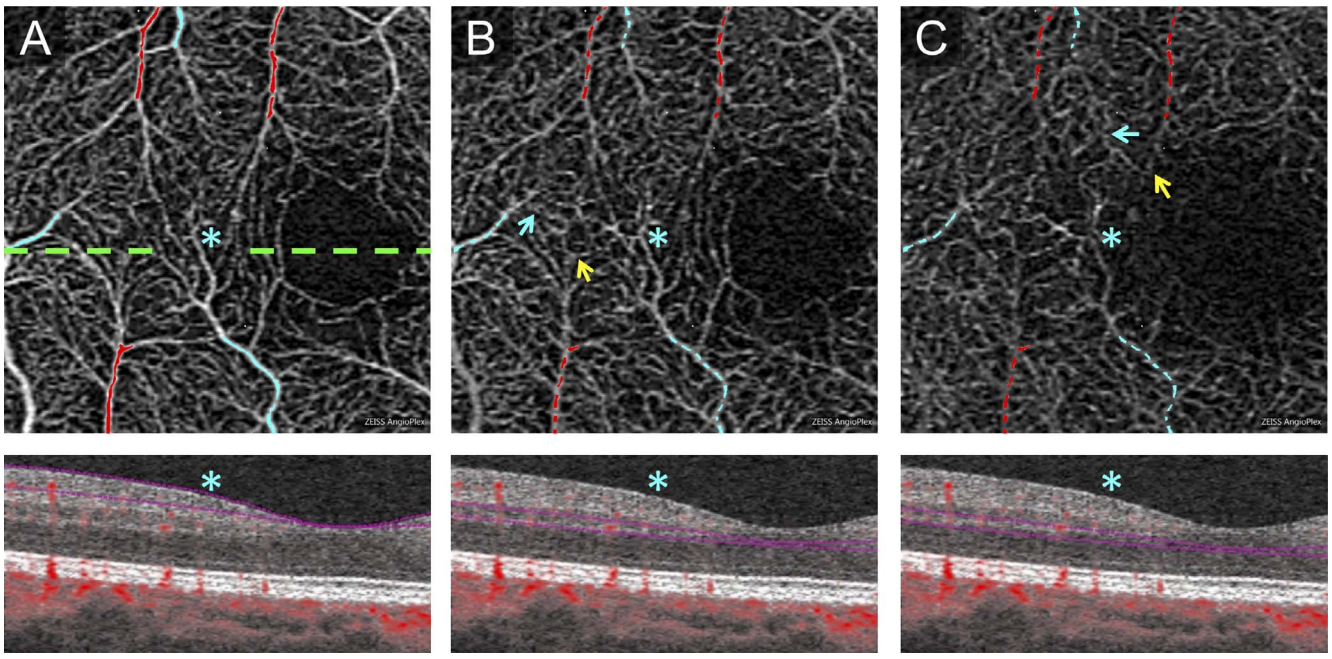

Figure 8. The "vortex" system connects to several arterioles and venules and crosses the horizontal raphe in the DCP. (**A**) En face OCTA of the SCP with arterioles (pseudo-colored *red*) and venules (pseudo-colored *blue*). Cross-sectional OCT below each angiogram with *purple segmentation boundaries* and *red flow overlay. Dotted line* shows location of cross-sections for (**A–C**). *Asterisks* highlight the location of the central conduit of the "vortex" connection to a venule. (**B**, **C**) Thin slabs (30 μm) of the DCP taken progressively deeper into the retina. (**B**) The vortex fans out in a radial fashion with connections to both arterioles (*yellow arrow*) and venules (*blue arrow*). (**C**) Vortex connection crosses the horizontal raphe and connects to superior arterioles (*yellow arrow*) and venules (*blue arrow*).

Investigative Ophthalmology & Visual Science

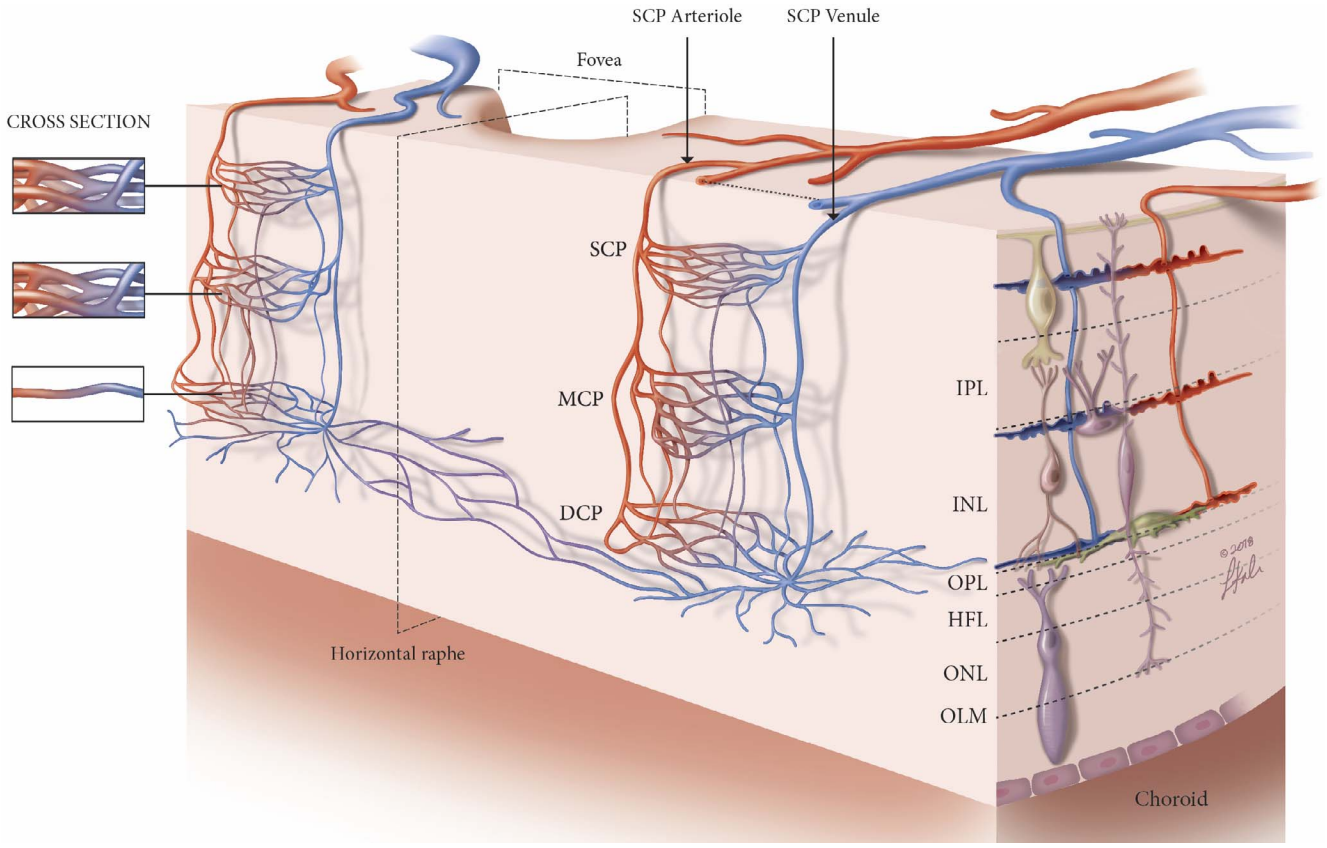

Figure 9. Proposed three-dimensional illustration of connectivity and configuration of the retina vascular plexuses. The SCP, MCP, and DCP receive their own arteriolar supply (*red*) from SCP arterioles, and show distinct venular drainage (*blue*) to SCP venules. Arterioles in the SCP are located on a more superficial plane than neighboring venules. The SCP is located mainly in the ganglion cell layer, as seen on the right, whereas the MCP and DCP are located at the top and bottom borders of the INL, respectively. In the cross-sectional view on the left, the three-dimensional complex architecture of the SCP and MCP is compared to the flat, laminar structure of the DCP. Direct anastomotic connections between each of these layers are seen on both the arteriolar and venular sides of the capillary beds. The DCP includes vortices that drain centrally into a venule, and also connect to other venules and arterioles through radially oriented capillaries. The DCP contains channels that traverse the horizontal raphe. HFL, Henle fiber layer; OLM, outer limiting membrane; ONL, outer nuclear layer.

dimensional complexity of the SCP and MCP capillaries, compared with the flat configuration of the DCP, which has been shown in human histologic studies.[1,48]

Strengths of our study include the use of OMAG software, which provides better axial resolution than split-spectrum algorithms, along with our use of en face and cross-sectional OCTA to trace the macular capillary connections in three dimensions. Whereas OMAG improves the axial resolution, the lateral resolution is not improved substantially, which can be considered a limitation of this study. Another limitation was the relatively small number of eyes. Future quantitative and detailed human histological studies are needed to examine the extent of arteriolar and venular connection to each of the capillary plexuses, and will be important to complement our understanding of the retinal vascular anatomy based on OCTA. Compared with histology, OCTA provides a dynamic measurement in vivo of channels that have flow above the threshold of detection, presumably functional vessels with active blood flow. The extent of functional capillaries is actively modified through autoregulation and reflects neurovascular coupling during flicker stimulation or stress.[19,49–51] This could explain the findings of higher retinal vascular density in histological methods compared with OCTA studies, as some capillaries may only be recruited (and have blood flow) during certain physiologic states.[48,52] We used the Angioplex "Remove Projections" function, which uses additive mixing of overlying vessels to remove projections in the lower layers. Future studies are needed to assess the strengths and weakness of the using Angioplex artifact removal software compared with PR-OCTA software or the projection artifact removal (PAR) software used by Optovue.

In conclusion, using OCTA software with relatively high axial resolution, we have identified connections between large superficial arterioles and venules and each of the retinal capillary plexuses (SCP, MCP, and DCP). We provide further evidence that SCP arterioles are located on a more superficial plane than neighboring venules. We propose a new, more comprehensive model of the connectivity and overall anatomy of the parafoveal retinal vascular layers, using our data and incorporating elements from previous studies.[1,8,9,16,17,30,31,43,46–48] This model and our data illustrate the complexity of capillary connections in the macula and would provide a great degree of redundancy and overlap that is necessary to support the high metabolic demand and specialized visual functions of the individual human macular neurovascular units.

Acknowledgments

The authors thank Gregory W. Schwartz, PhD, Feinberg School of Medicine, Northwestern University, for his insightful discussions about this manuscript, and Lauren Kalinoski, MS, for her artistic contributions to the schematic illustration in Figure 9.

Supported by National Institutes of Health Grant DP3DK108248 (AAF), by a Research to Prevent Blindness Award to Northwestern University Department of Ophthalmology, and research instrument support by Zeiss Meditec, Inc. (Dublin, CA, USA). The authors alone are responsible for the content and writing of this paper.

Disclosure: **P.L. Nesper**, None; **A.A. Fawzi**, None

References

1. Chan G, Balaratnasingam C, Paula KY, et al. Quantitative morphometry of perifoveal capillary networks in the human retina. *Invest Ophthalmol Vis Sci*. 2012;53:5502–5514.
2. Tan PEZ, Paula KY, Balaratnasingam C, et al. Quantitative confocal imaging of the retinal microvasculature in the human retina. *Invest Ophthalmol Vis Sci*. 2012;53:5728–5736.
3. Provis JM. Development of the primate retinal vasculature. *Prog Retin Eye Res*. 2001;20:799–821.
4. Gariano RF, Iruela-Arispe ML, Hendrickson AE. Vascular development in primate retina: comparison of laminar plexus formation in monkey and human. *Invest Ophthalmol Vis Sci*. 1994;35:3442–3455.
5. Snodderly DM, Weinhaus RS, Choi J. Neural-vascular relationships in central retina of macaque monkeys (*Macaca fascicularis*). *J Neurosci*. 1992;12:1169–1193.
6. Snodderly DM, Weinhaus RS. Retinal vasculature of the fovea of the squirrel monkey, *Saimiri sciureus*: three-dimensional architecture, visual screening, and relationships to the neuronal layers. *J Comp Neurol*. 1990;297:145–163.
7. Weinhaus RS, Burke JM, Delori FC, Snodderly DM. Comparison of fluorescein angiography with microvascular anatomy of macaque retinas. *Exp Eye Res*. 1995;61:1–16.
8. Park JJ, Soetikno BT, Fawzi AA. Characterization of the middle capillary plexus using optical coherence tomography angiography in healthy and diabetic eyes. *Retina*. 2016;36:2039–2050.
9. Campbell J, Zhang M, Hwang T, et al. Detailed vascular anatomy of the human retina by projection-resolved optical coherence tomography angiography. *Sci Rep*. 2017;7:42201.
10. Hwang TS, Zhang M, Bhavsar K, et al. Visualization of 3 distinct retinal plexuses by projection-resolved optical coherence tomography angiography in diabetic retinopathy. *JAMA Ophthalmol*. 2016;134:1411–1419.
11. Chu S, Nesper PL, Soetikno BT, Bakri S, Fawzi AA. Projection-resolved OCT angiography of microvascular changes in paracentral acute middle maculopathy and acute macular neuroretinopathy. *Invest Ophthalmol Vis Sci*. 2018;59:2913–2922.
12. Chan G, Balaratnasingam C, Xu J, et al. In vivo optical imaging of human retinal capillary networks using speckle variance optical coherence tomography with quantitative clinico-histological correlation. *Microvasc Res*. 2015;100:32–39.
13. Kurokawa K, Sasaki K, Makita S, et al. Three-dimensional retinal and choroidal capillary imaging by power Doppler optical coherence angiography with adaptive optics. *Opt Express*. 2012;20:22796–22812.
14. Salas M, Augustin M, Ginner L, et al. Visualization of micro-capillaries using optical coherence tomography angiography with and without adaptive optics. *Biomed Opt Express*. 2017;8:207–222.
15. Felberer F, Rechenmacher M, Haindl R, et al. Imaging of retinal vasculature using adaptive optics SLO/OCT. *Biomed Opt Express*. 2015;6:1407–1418.
16. Bonnin S, Mané V, Couturier A, et al. New insight into the macular deep vascular plexus imaged by optical coherence tomography angiography. *Retina*. 2015;35:2347–2352.
17. Garrity ST, Paques M, Gaudric A, Freund KB, Sarraf D. Considerations in the understanding of venous outflow in the retinal capillary plexus. *Retina*. 2017;37:1809–1812.
18. Biesecker KR, Srienc AI, Shimoda AM, et al. Glial cell calcium signaling mediates capillary regulation of blood flow in the retina. *J Neurosci*. 2016;36:9435–9445.
19. Kornfield TE, Newman EA. Regulation of blood flow in the retinal trilaminar vascular network. *J Neurosci*. 2014;34:11504–11513.
20. Hagag AM, Pechauer AD, Liu L, et al. OCT angiography changes in the 3 parafoveal retinal plexuses in response to hyperoxia. *Ophthalmol Retina*. 2017;2:329–336.
21. Jia Y, Tan O, Tokayer J, et al. Split-spectrum amplitude-decorrelation angiography with optical coherence tomography. *Opt Express*. 2012;20:4710–4725.
22. Gao SS, Liu G, Huang D, Jia Y. Optimization of the split-spectrum amplitude-decorrelation angiography algorithm on a spectral optical coherence tomography system. *Opt Lett*. 2015;40:2305–2308.
23. An L, Shen TT, Wang RK. Using ultrahigh sensitive optical microangiography to achieve comprehensive depth resolved microvasculature mapping for human retina. *J Biomed Opt*. 2011;16:106013.
24. Wang RK, An L, Francis P, Wilson DJ. Depth-resolved imaging of capillary networks in retina and choroid using ultrahigh sensitive optical microangiography. *Opt Lett*. 2010;35:1467–1469.
25. Rosenfeld PJ, Durbin MK, Roisman L, et al. Zeiss Angioplex™ spectral domain optical coherence tomography angiography: technical aspects. In: Bandello F, Souied EH, Querques G. *OCT Angiography in Retinal and Macular Diseases*. Basel, Switzerland: Karger Publishers; 2016:18–29.
26. Chylack LT, Wolfe JK, Singer DM, et al. The lens opacities classification system III. *Arch Ophthalmol*. 1993;111:831–836.
27. Zhang Q, Lee CS, Chao J, et al. Wide-field optical coherence tomography based microangiography for retinal imaging. *Sci Rep*. 2016;6:22017.
28. Zhang Q, Huang Y, Zhang T, et al. Wide-field imaging of retinal vasculature using optical coherence tomography-based microangiography provided by motion tracking. *J Biomed Opt*. 2015;20:066008.
29. Bagherinia H, Knighton RW, De Sisternes L, et al. A fast method to reduce decorrelation tail artifacts in OCT angiography. *Invest Ophthalmol Vis Sci*. 2017;58:643–643.
30. Toussaint D, Kuwabara T, Cogan DG. Retinal vascular patterns: part II. Human retinal vessels studied in three dimensions. *Arch Ophthalmol*. 1961;65:575–581.
31. Savastano MC, Lumbroso B, Rispoli M. In vivo characterization of retinal vascularization morphology using optical coherence tomography angiography. *Retina*. 2015;35:2196–2203.
32. Dorrell MI, Aguilar E, Friedlander M. Retinal vascular development is mediated by endothelial filopodia, a preexisting astrocytic template and specific R-cadherin adhesion. *Invest Ophthalmol Vis Sci*. 2002;43:3500–3510.
33. Usui Y, Westenskow PD, Kurihara T, et al. Neurovascular crosstalk between interneurons and capillaries is required for vision. *J Clin Invest*. 2015;125:2335–2346.
34. Yu D, Cringle S, Alder V, Su E. Intraretinal oxygen distribution in rats as a function of systemic blood pressure. *Am J Physiol Heart Circ Physiol*. 1994;267:H2498–H2507.
35. Yu D-Y, Cringle SJ, Su E-N. Intraretinal oxygen distribution in the monkey retina and the response to systemic hyperoxia. *Invest Ophthalmol Vis Sci*. 2005;46:4728–4733.
36. Cringle SJ, Yu D-Y, Paula KY, Su E-N. Intraretinal oxygen consumption in the rat in vivo. *Invest Ophthalmol Vis Sci*. 2002;43:1922–1927.
37. Yu D-Y, Cringle SJ, Alder V, Su E-N. Intraretinal oxygen distribution in the rat with graded systemic hyperoxia and hypercapnia. *Invest Ophthalmol Vis Sci*. 1999;40:2082–2087.

Investigative Ophthalmology & Visual Science

38. Yu D-Y, Cringle SJ, Paula KY, Su E-N. Intraretinal oxygen distribution and consumption during retinal artery occlusion and graded hyperoxic ventilation in the rat. *Invest Ophthalmol Vis Sci*. 2007;48:2290–2296.
39. Linsenmeier RA, Zhang HF. Retinal oxygen: from animals to humans. *Prog Retin Eye Res*. 2017;58:115–151.
40. Lau JC, Linsenmeier RA. Oxygen consumption and distribution in the Long-Evans rat retina. *Exp Eye Res*. 2012;102:50–58.
41. Padnick-Silver L, Derwent JJK, Giuliano E, et al. Retinal oxygenation and oxygen metabolism in Abyssinian cats with a hereditary retinal degeneration. *Invest Ophthalmol Vis Sci*. 2006;47:3683–3689.
42. Birol G, Wang S, Budzynski E, et al. Oxygen distribution and consumption in the Macaque retina. *Am J Physiol Heart Circ Physiol*. 2007;293:H1696–H1704.
43. Gorczynska I, Migacz JV, Zawadzki RJ, et al. Comparison of amplitude-decorrelation, speckle-variance and phase-variance oct angiography methods for imaging the human retina and choroid. *Biomed Opt Express*. 2016;7:911–942.
44. Fouquet S, Vacca O, Sennlaub F, Paques M. The 3D retinal capillary circulation in pigs reveals a predominant serial organization. *Invest Ophthalmol Vis Sci*. 2017;58:5754–5763.
45. Genevois O, Paques M, Simonutti M, et al. Microvascular remodeling after occlusion-recanalization of a branch retinal vein in rats. *Invest Ophthalmol Vis Sci*. 2004;45:594–600.
46. Paques M, Tadayoni R, Sercombe R, et al. Structural and hemodynamic analysis of the mouse retinal microcirculation. *Invest Ophthalmol Vis Sci*. 2003;44:4960–4967.
47. Leahy C, Radhakrishnan H, Weiner G, et al. Mapping the 3D connectivity of the rat inner retinal vascular network using OCT angiography. *Invest Ophthalmol Vis Sci*. 2015;56:5785–5793.
48. Balaratnasingam C, An D, Sakurada Y, et al. Comparisons between histology and optical coherence tomography angiography of the periarterial capillary-free zone. *Am J Ophthalmol*. 2018;189:55–64.
49. Crawford JH, Isbell TS, Huang Z, et al. Hypoxia, red blood cells, and nitrite regulate no-dependent hypoxic vasodilation. *Blood*. 2006;107:566–574.
50. Rassam S, Patel V, Chen H, Kohner E. Regional retinal blood flow and vascular autoregulation. *Eye*. 1996;10:331.
51. Duan A, Bedggood PA, Bui BV, Metha AB. Evidence of flicker-induced functional hyperaemia in the smallest vessels of the human retinal blood supply. *PLoS One*. 2016;11:e0162621.
52. An D, Balaratnasingam C, Heisler M, et al. Quantitative comparisons between optical coherence tomography angiography and matched histology in the human eye. *Exp Eye Res*. 2018;170:13–19.

Investigative Ophthalmology & Visual Science